

## Deformation Textures in fcc Metals Subjected to Frictional and to Abrasive Wear

Robert A. Schwarzer

Institute of Physics, TU Clausthal, D-38678 Clausthal-Zellerfeld, Germany

schwarzer@tu-clausthal.de

**Keywords:** Abrasion texture, wear texture, X-ray pole figures, SAD pole figures, ODF

**Abstract.** The surface texture in fcc metals has been investigated after wear tests in a dry-running pin-on-disk test machine and after metallographic surface grinding. X-ray pole figures have been measured at a low angle of incidence of the primary beam, using an area detector for recording the diffraction patterns. SAD pole figures have been acquired on cross sections on-line in the TEM in order to examine the gradient of texture and microstructure beneath the surface. The XRD and SAD pole figures have been evaluated by ODF calculation. Wear and abrasion textures are distinctly different both for copper and bronze as well as for brass.

### Introduction

Deformation textures have been subjected to extensive experimental and theoretical investigations in the literature since decades. The formation of the rolling texture in sheet metals is of particular technical importance. It is quite well understood for the mid plane, but the models to predict the gradual change of texture from the center to the surface of the sheet and of the surface texture itself need still some attention. In addition to almost planar compression in sheet normal direction, a shear effect of increasing intensity from the center to the sheet surface has to be taken into account, depending on the ratio of roll diameter to stitch, speed, the lubricant and the friction between the sheet and the rolls. Furthermore, wear and shear are the dominating deformation processes in bearings, wheel-rail-systems and in superfinishing surfaces. Nevertheless, shear texture has been studied less frequently than rolling texture.

### Experimental

The wear experiments of this investigation have been performed with a pin-on-disk apparatus on air without lubricant. Pins and disks were made of the same material – pure copper and bronze, respectively  $\alpha$  brass – to avoid phase mixing which might affect adversely the analysis of the diffraction patterns. The pin diameters were 6 mm, the load on the pins ranged from 0.2 to 1 N, and the slide speed was about 5 mm/sec. After a short run of less than 15 min, the initially polished surfaces of contact became rough, in particular with pure copper. The final textures were reached after about 30 min to one hour of wear test.

The abrasion samples were ground for about 5 min on a rotating disk covered with Al<sub>2</sub>O<sub>3</sub> paper in grades of 600, 800, 1000 respectively 1200 mesh. As is the usual procedure in metallography, the disk was permanently rinsed with water to cool the samples and to remove debris. However, only a light pressure (about 300 N/m<sup>2</sup>) was applied by hand to the samples, and the samples were held in a stationary position on the rotating disk in order to achieve unidirectional abrasion. As observed visually, the abraded surfaces were traversed relatively uniformly by fine scratches aligned parallel with the direction of abrasion. Finally, the samples were cleaned in an ultrasonic bath with ethanol. No etching whatsoever was applied.

Texture measurement was performed by X-ray and electron diffraction. The X-ray pole figures were acquired in reflection with Co K $\alpha$  radiation using a Bruker GADDS area detector. To estimate the homogeneity of shear texture in depth beneath the surface, two series of measurement were carried out on the same samples, one at an angle of incidence of 15° and the other one at 30° to the

surface. The flat incidence of the primary X-ray beam increases sensitivity to the surface layer, whereas 30° are adequate to probe the transition between the deformed layer and the initial sheet structure. It is worth noting that pole figure measurement using an area detector is performed with a primary X-ray beam at a constant angle of incidence. The sample is only rotated about its normal and maintained at a constant tilt angle. Therefore, the penetration depth is the same for all pole figure points and all pole figures of one acquisition setup.

The highest surface sensitivity can be achieved by grazing incidence SAD pole figure measurement in the TEM [1]. The wear-tested as well as the abraded surfaces, however, were too rough for reflection electron diffraction whereby the samples have to be rotated about their normal direction, ND, during measurement. Therefore, cross-sections perpendicular to the original surfaces were prepared by fixing samples surface-on-surface with a low-melting point solder, dimple-grinding and finally electropolishing the sections to transparency for 200 kV electrons at the surfaces of contact. As a result the original surfaces were neither in touch with nor affected by the electrolyte. These surfaces were aligned parallel with the electron beam and perpendicular to the tilt axis of the side entry goniometer of the TEM. By tilting the samples in small angular steps of 5° from -50° to +50° about the goniometer axis, series of SAD diffraction patterns were acquired with a digital CCD camera (Gatan 794 MSC) from selected small areas. The probed areas ranged from 5 µm to 50 µm beneath the surface, depending on the local roughness of the contact surfaces.

## Results

From the digital XRD and the SAD patterns, the ODF and pole figures have been calculated using the iterative series expansion method [2, 3]. In spite of the much lower statistics in SAD, the main peaks in the SAD pole figures are in agreement with those in the XRD pole figures at flat incidence. It is worth noting that the XRD pole figures indicate the development of a sample symmetry very close to *monoclinic* during surface wear as well as grinding and polishing, as contrasted to an almost orthorhombic sample symmetry which is usually produced in the mid plane of sheet metals during deformation by rolling in one direction. The mirror plane in the SD-ND plane reflects the symmetry of the deformation process in the direction of planar shear, SD. Although the ODF has been calculated under the assumption of triclinic sample symmetry, for convenience only the monoclinic sections of the ODF are presented in the following figures.

**a. Wear.** Copper and bronze develop a very similar wear texture. The maximum in the ODF is located at  $(\varphi_1 = 45^\circ, \Phi = 60^\circ, \varphi_2 = 75^\circ) \approx (5\ 1\ 3)[-1\ -4\ 3]$ . Further main components are at  $(\varphi_1 = 15^\circ, \Phi = 60^\circ, \varphi_2 = 60^\circ) \approx (3\ 2\ 2)[2\ -4\ 1]$  and  $(\varphi_1 = 40^\circ, \Phi = 45^\circ, \varphi_2 = 45^\circ) \approx (2\ 2\ 3)[1\ -4\ 2]$  (Fig. 1).

The wear texture of brass (Fig. 2) is significantly different from that of copper. It can be approximated by the main components at  $(\varphi_1 = 85^\circ, \Phi = 90^\circ, \varphi_2 = 45^\circ) \approx (1\ 1\ 0)[1\ -4\ 7]$  (maximum),  $(\varphi_1 = 0^\circ, \Phi = 45^\circ, \varphi_2 = 0^\circ) \approx (0\ 1\ 1)[1\ 0\ 0]$ ,  $(\varphi_1 = 35^\circ, \Phi = 90^\circ, \varphi_2 = 0^\circ) \approx (0\ 1\ 0)[3\ 0\ 2]$  and  $(\varphi_1 = 60^\circ, \Phi = 45^\circ, \varphi_2 = 45^\circ) \approx (2\ 2\ 3)[-1\ -5\ 4]$ . Texture gradually changes with depth beneath the surface, as can be seen by comparing Fig. 2 (15° angle of incidence) with Fig. 3 obtained at 30° angle of incidence of the primary X-ray beam. The texture of the deeper surface layer contains the following main components:  $(\varphi_1 = 0^\circ, \Phi = 55^\circ, \varphi_2 = 70^\circ) \approx (4\ 1\ 3)[1\ -4\ 0]$  (maximum),  $(\varphi_1 = 0^\circ, \Phi = 45^\circ, \varphi_2 = 0^\circ) \approx (0\ 1\ 1)[1\ 0\ 0]$ ,  $(\varphi_1 = 35^\circ, \Phi = 90^\circ, \varphi_2 = 0^\circ) \approx (0\ 1\ 0)[3\ 0\ 2]$ ,  $(\varphi_1 = 25^\circ, \Phi = 55^\circ, \varphi_2 = 45^\circ) \approx (111)[3\ -5\ 2]$  and  $(\varphi_1 = 50^\circ, \Phi = 55^\circ, \varphi_2 = 45^\circ) \approx (111)[1\ -5\ 4]$ .

**b. Abrasion.** The surface texture of abraded copper and bronze sheets (Fig. 4) differs significantly from a wear texture. It contains the main components at  $(\varphi_1 = 0^\circ, \Phi = 90^\circ, \varphi_2 = 5^\circ) \approx (0\ 1\ 0)[1\ 0\ 0]$  (maximum),  $(\varphi_1 = 30^\circ, \Phi = 45^\circ, \varphi_2 = 0^\circ) \approx (0\ 1\ 1)[3\ -1\ 1]$  and  $(\varphi_1 = 25^\circ, \Phi = 40^\circ, \varphi_2 = 35^\circ) \approx (3\ 4\ 6)[2\ -3\ 1]$ .

The abrasion texture of brass can be approximated by two main components at  $(\varphi_1 = 30^\circ, \Phi = 45^\circ, \varphi_2 = 0^\circ) \approx (0\ 1\ 1)[5\ -2\ 2]$  (maximum) and  $(\varphi_1 = 60^\circ, \Phi = 25^\circ, \varphi_2 = 65^\circ) \approx (2\ 1\ 5)[-4\ -7\ 3]$  (Fig. 5). It differs significantly from the abrasion texture of copper and bronze.

**c. Observations in the TEM.** Due to the small diffracting volume in SAD diffraction, TEM pole figures appeared coarse grained with low statistics. The main peaks, however, agree reasonably well with the XRD pole figures at flat incidence. The investigation of the abraded and the wear surfaces by imaging and diffraction in the TEM gave no evidence of an amorphous surface layer (“Beilby layer”, [4]). The depth of deformation ranged from about 100  $\mu\text{m}$  with coarse grade abrasion paper to 20  $\mu\text{m}$  on flat wear surfaces or after abrasion with 1200 grade aluminum oxide paper.

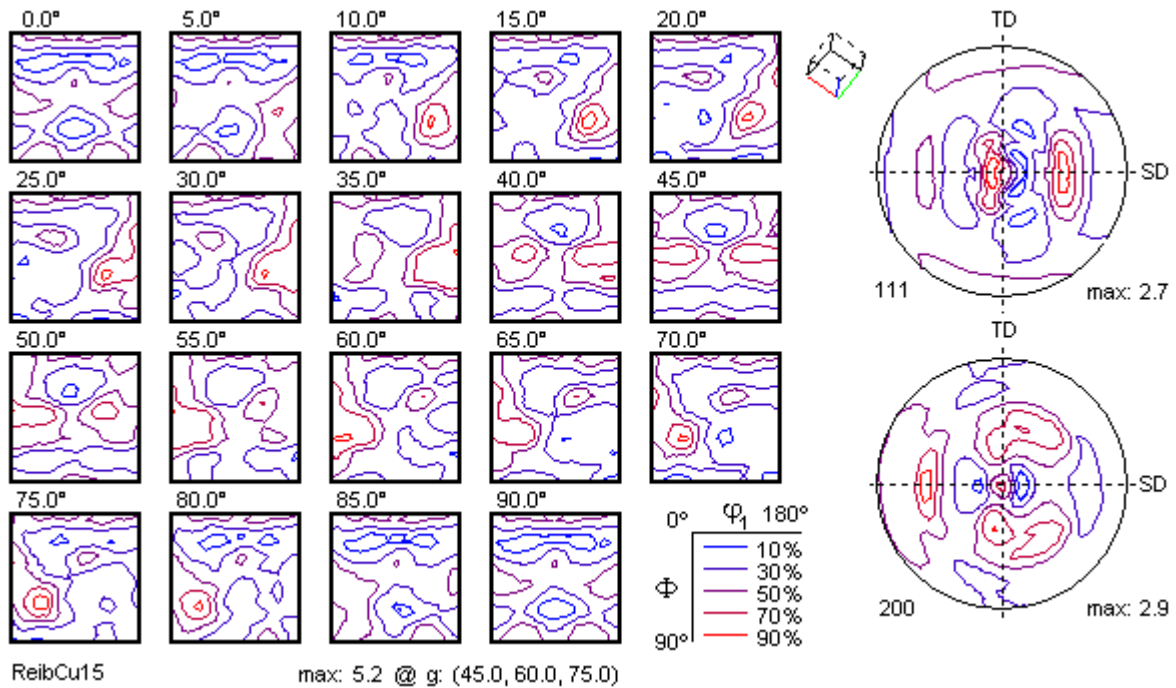


Figure 1 The wear texture of copper at 15° angle of incidence of the X-ray beam.

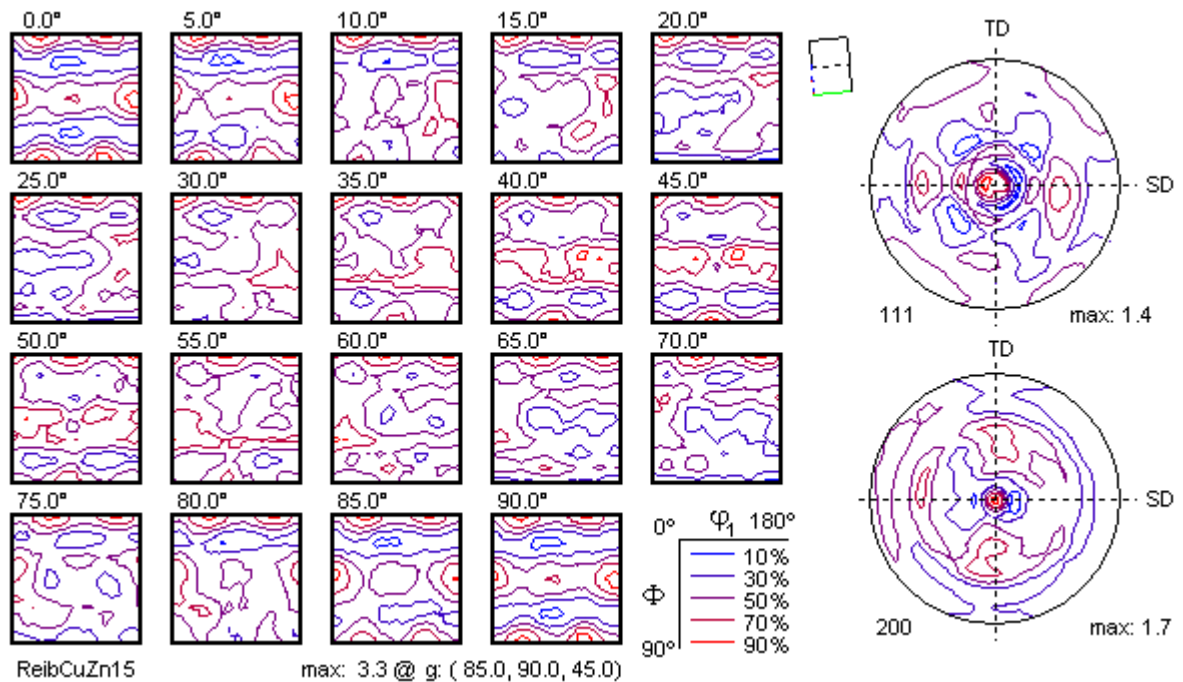


Figure 2 The wear texture of brass at 15° angle of incidence of the X-ray beam.

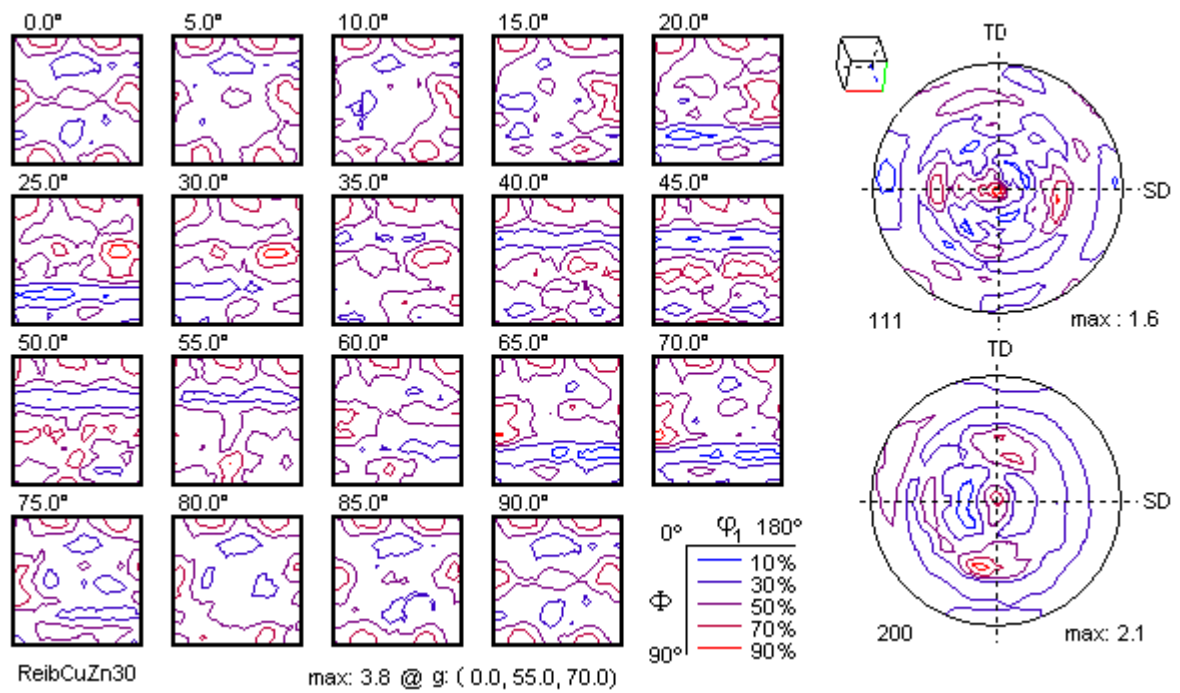


Figure 3 The wear texture of brass at 30° angle of incidence of the X-ray beam.

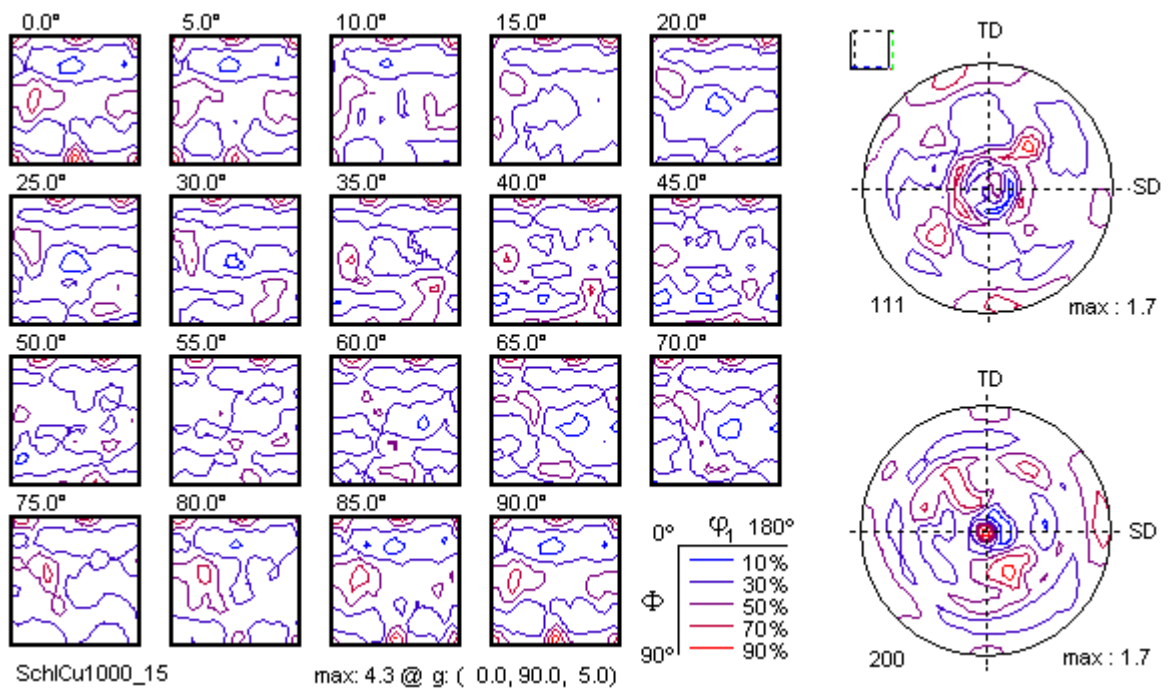


Figure 4 The abrasion texture of copper at 15° angle of incidence of the X-ray beam.

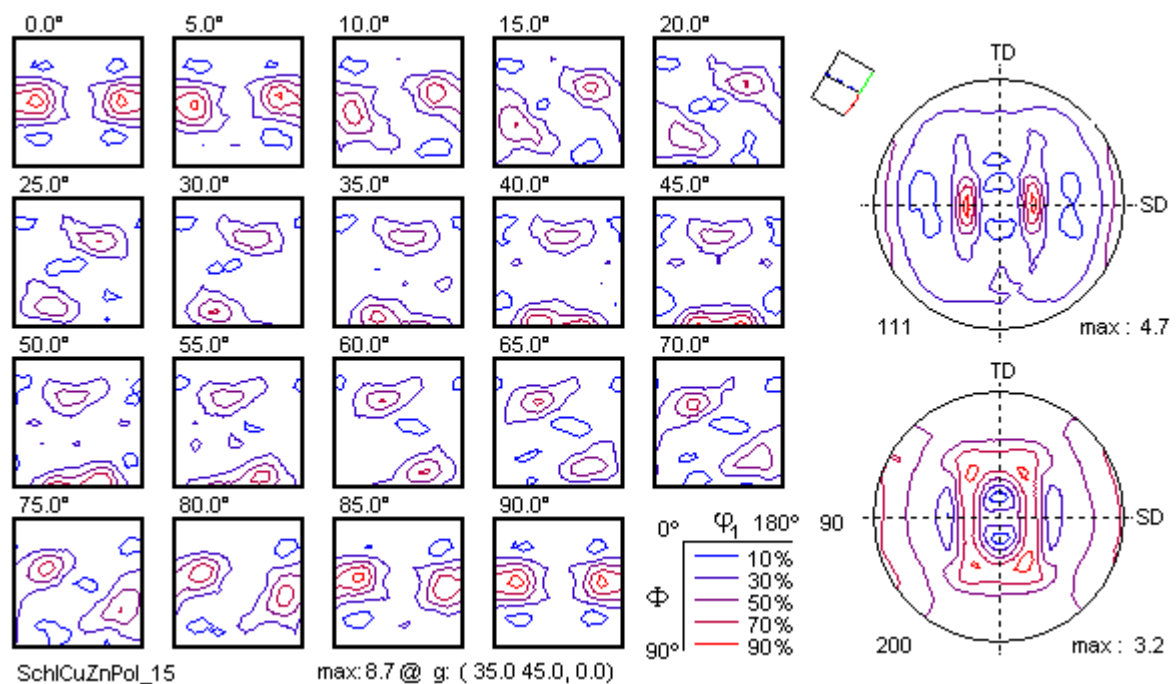


Figure 5 The abrasion texture of brass at 15° angle of incidence of the X-ray beam.

## Discussion

For a better understanding of the wear mechanisms of the wheel-rail-system, the shear textures of fcc metals have been measured after asymmetric rolling [5, 6]. The (111) pole figures of the final texture of copper agree fairly well with our findings. The components have been interpreted on the basis of one single experimental pole figure as to contain preferred orientations close to (111)[0-11] and (111)[01-1], whereby [111] is tilted by  $-10^\circ$  respectively  $+50^\circ$  from the sheet normal to the direction of slide, and a (001)[1-10] component of a about half the intensity.

Wear texture has not yet been studied intensively in literature. A symmetrical (111) pole figure of rolled copper is shown in [7]. It reflects an orthorhombic symmetry and differs from the results obtained in the present investigation. The authors admit that the “main peaks of the rolling texture may shine through”. The (111) pole figures of torsion tests in the same paper and Figure 7b in [8] have two peaks on the shear direction. They roughly agree with our findings. The shear texture of brass for torsion tests has been calculated with the Taylor theory by taking mechanical twinning on  $\{111\}\langle 112 \rangle$  into account [9]. The results differ considerably from our experimental findings. One reason for this discrepancy might be the suppression of twinning in very small grains which are formed in the surface of wear. In addition, the geometries of torsion tests and sliding wear are too different to expect the formation of the same type of deformation textures. The evolution of surface texture in low-carbon steels during machining by abrasives and superfinishing has been investigated in [10].

The geometries associated with wear, abrasion, torsion tests and sheet rolling are not the same so that different textures are developed. In frictional wear, the shear force is unidirectional in the plane of slide, exerting compression in tangential direction. Local inhomogeneities arise when the surfaces of contact start cold-welding or if debris is not removed. Grinding and polishing involves removing, cutting and turning up material like plowing. Shear forces are exerted not only in one direction in the surface plane, but also in cross-direction on the side-walls of the grooves. In wear, grinding and polishing, a static force is furthermore applied in normal direction by the load. Torsion tests on solid cylinders, however, result in a strain gradient from the surface (maximum shear) to the center (no shear). The surface of cylinders or tubes need to be flattened for XRD pole figure

measurement which induces additional strain. There are no stable orientations during torsion because any particular grain is constantly rotating with no definite stationary end-points in orientation space.

## Summary

- There is no evidence of an amorphous surface layer (“Beilby layer”) after frictional wear.
- The (111), (200) and (220) pole figures are symmetrical about the directions of friction respectively of abrasion. A monoclinic rather than an orthorhombic sample symmetry has evolved.
- After wear tests, copper and bronze surfaces show a very similar, characteristic “copper wear texture”. The “wear texture of brass” is distinctly different from the copper wear texture.
- After metallographic grinding on aluminum oxide abrasive paper of various grades and water lubrication, a fine grain polycrystalline microstructure is seen on the sample surfaces. Two distinct textures have developed again, one typical for copper and bronze, and the other for brass. The abrasion texture of brass does not change significantly with finer grain size of the abrasive.

In conclusion, texture can be used as a fingerprint to analyze failures of a workpiece, because frictional wear and abrasion produce different and significant textures at the surfaces. Potential applications of surface wear or abrasion are the fabrication of specific surface textures for deposition substrates and protection layers with improved adhesion. Textures and properties of thin sheet metals may be modified by giving a brush or grinding to the surfaces, followed by a controlled recrystallization heat treatment.

## Acknowledgment

Financial support by the German Research Foundation under DFG project SCHW 403/13-1 is gratefully acknowledged. The author thanks Mr. Jörg Schumann for assisting the experiments.

## References

- [1] B. Schäfer and R.A. Schwarzer: SAD pole figures in transmission and reflection using a high-grade CCD camera as an area detector. *Mater. Sci. Forum* Vol. **273-275** (1998), pp. 223-228
- [2] M. Dahms and H.J. Bunge: The iterative series expansion method for quantitative texture analysis. I. General outline. *J. Appl. Cryst.* Vol. **22** (1989), pp. 439-447
- [3] B. Schäfer: ODF computer program for high-resolution texture analysis with low-symmetry materials. *Mater. Sci. Forum* Vol. **273-275** (1998), pp. 113-118
- [4] L.E. Samuels: *Metallographic Polishing by Mechanical Methods*. 3<sup>rd</sup> Edition. American Society for Metals, Metals Park 1985
- [5] H. Krause and A.H. Demirci: Final texture of copper subjected to frictional stresses. *Wear* Vol. **37** (1976), pp. 53-61
- [6] H. Krause and A.H. Demirci: Texture changes in the running surface of face-centered cubic metals as the result of frictional stress. *Wear* Vol. **61** (1980), pp. 325-332
- [7] P.J. Regenet and H.P. Stüwe: Zur Entstehung von Oberflächentexturen beim Walzen kubisch flächenzentrierter Metalle. *Z. Metallkunde* Vol. **54** (1963), pp. 273-278
- [8] J. Gil-Sevillano, P. Van Houtte and E. Aernoudt: Die Deutung der Schertexturen mit Hilfe der Taylor-Analyse. *Z. Metallkunde* Vol. **66** (1975), pp. 367-373
- [9] P. Van Houtte: Simulation of the rolling and shear texture of brass by the Taylor theory adapted for mechanical twinning. *Acta Metallurgica* Vol. **26** (1978), pp. 591-604
- [10] V.I. Savchuk, I.A. Moroz, V.S. Ivaniji and A.V. Grishkevich: Textures forming in some steels machined by abrasives. *Kristall und Technik* Vol. **14** (1979), pp. 471-474